Computational Fluid Dynamic Investigations of Propeller Cavitation in the Presence of a Rudder

Naz Yilmaz*, Mehmet Atlar*, Patrick A. Fitzsimmons*, Noriyuki Sasaki*

***University of Strathclyde, Glasgow, UK**, naz.gorener@strath.ac.uk, mehmet.atlar@strath.ac.uk, patrick.a.fitzsimmons@gmail.com, noriyuki.sasaki@strath.ac.uk

Abstract

This paper presents the preliminary results of a computational study for cavitation modelling of marine propellers particularly developing tip vortex cavitation in the presence of a rudder. The main purpose of the study is to estimate the propeller's performance in cavitating conditions and to investigate the propeller-rudder interaction especially due to the tip-vortex cavitation. The cavitation simulations were conducted using commercial Computational Fluid Dynamics (CFD) software, Star CCM+. In the study, the INSEAN E779A model propeller was used as a benchmark. Firstly, validation studies were conducted in cavitating conditions using only the propeller in isolation. The cavitation on the propeller was simulated by using a numerical model, which is known as Schnerr–Sauer cavitation model, based on the Rayleigh-Plesset equation. Then, the rudder with an airfoil section was introduced behind the propeller and the simulations were repeated to investigate the effect of the rudder on the propeller performance as well as to study the propeller-rudder interaction from the cavitation point of view. Two cases with different advance coefficients (J) and cavitation numbers (σ) were simulated to compare the computational results with experiments which were obtained from open literature. For the tip vortex cavitation modelling, recently developed volumetric control method using spiral geometry was applied to generate finer mesh around the propeller tip region where the tip vortex cavitation may occur. The comparison with the benchmark experimental data showed good agreement in terms of thrust and torque coefficients as well as sheet and tip vortex cavitation patterns for the propeller in the absence of the rudder. The comparisons also showed good agreement in terms of the velocity and pressure distributions and hence enabled accurate extension of the tip vortex cavitation until the rudder to focus on the interaction of the tip vortex cavitation with the rudder.

Keywords: Propeller Cavitation, CFD, Propeller-Rudder Interaction, Tip Vortex Cavitation, DES, LES

1. Introduction

Cavitation is a complex phenomenon which may affect the performance of a ship's propeller in an unfavourable way resulting in efficiency loss, blade erosion, fluctuating hull vibration as well as underwater radiated noise. There are different types of cavitation such as sheet, bubble, cloud, tip and hub vortex cavitation (Carlton, 2007). Each type of cavitation affects the propeller performance differently. Some sheet cavitation is associated with erosive effects on propeller blade surfaces, tip vortex cavitation is important for radiated noise particularly for naval, survey and cruise ships; it can also cause erosion on and behind the leading edge of the rudder. Therefore, the cavitation occurrences should be investigated for marine propellers. Although the propeller cavitation is an essential phenomenon to predict the propeller's performance and evaluate its undesirable effects, its interaction with the rudder is also important and complex from both the propeller and rudder point of view and hence should be investigated for the propeller and rudder in combination.

The propeller-rudder interaction phenomenon may be investigated in two parts: (1) The intervention to the pressure distribution, where the propeller is operating in front of the rudder in the flow, by the rudder; (2) The effect of the propeller flow field on the rudder which sometimes manifests itself in cavitation erosion of the rudder structure (Carlton, 2007). These two parts may be investigated using existing numerical methods, experimental methods or experimental fluid dynamics (EFD) and computational fluid dynamics (CFD) methods thanks to developing computational power and technology.

In the past 10 years, the propeller-rudder interaction has been investigated experimentally by many researchers. Felli and his colleagues (Felli et al., 2008) conducted detailed flow measurement experiments on an isolated free-running propeller-rudder combination using the INSEAN E779A model propeller. They captured the tip vortex and rudder interaction in detail during the tests. Following these initial tests, the propeller tip and hub vortex dynamics were investigated using the same model propeller and rudder geometries in a different combination – propeller and rudder has been located at the same axial plane by contrast with the combination at Felli et al., 2008 – by Felli and Falchi (Felli and Falchi, 2011). The results of this latter test were used in this paper to compare with the CFD results presented in Section § 5.3.2.

In varying degrees, experimental methods, numerical and computational fluid dynamics methods have been also used to investigate the propeller-rudder interaction phenomena for many years. Han, et al. (Han et al., 2001) used numerical approach by mixing classical vortex lattice method with surface panel method to predict propeller cavitation interacting with a horn-type rudder. Natarajan developed an iterative method which coupled a finite volume method, a vortex-lattice method and, a boundary

element method for analysing marine propellers in cavitating conditions in the presence of a rudder (Natarajan, 2003). In the same year, Lee et al, presented a coupled method including a vortex lattice method, a finite volume method and boundary element method to predict rudder sheet cavitation, including interaction with the propeller and tunnel wall affects (Lee et al., 2003). Mutual hydrodynamic interaction between the propeller and rudder were investigated using numerical models including lifting surface and boundary element methods for representing propeller and rudder geometries respectively by Szantyr (Szantyr, 2007a). Szantyr has also investigated dynamic interaction of tip vortex cavitation with the rudder using a model which is based on the Rankine vortex and the potential solution of the cylindrical sections of the cavitating kernel passing through the strongly varying pressure distribution in the vicinity of the rudder leading edge (Szantyr, 2007b).

The main objective of this paper to make a further contribution into the understanding of the propeller-rudder interaction phenomenon from the cavitation point of view, particularly for tip vortex cavitation. CFD methods were used at model scale for investigation of this complex phenomenon.

Carlton investigated propeller-rudder-hull interaction using sea trails results, CFD studies for different rudder geometries and model tests. His study underlined the importance of rudder-propeller-hull interaction in terms of the flow characteristics around the rudder geometry and also the implications for the rudder's contribution to the overall propulsion efficiency (Carlton et al., 2009). Many investigations have been conducted by using CFD methods for better understanding of the cavitation phonemenon including the effect of rudder in terms of the sheet cavitation developed on the blades and tip vortex cavitation. Boorsma and Whitworth discussed improvements in cavitation prediction using CFD methods and their ability to predict small-scale motions in the flow using DES, which are important for determining the erosive potential of both sheet and vortex cavitation on propeller and rudder geometries respectively (Boorsma and Whitworth, 2011). Simulation of cavitating flow and hull pressure fluctuations have been realized using RANS methods to evaluate the propeller performance in behind-hull, cavitating conditions by Paik et al. (Paik, et al., 2013). These results showed good agreement in terms not only of the cavitation pattern, but also those of the hull pressure fluctuation induced by the propeller, when the simulation results were compared with corresponding experiments carried out in Samsung Cavitation Tunnel (SCAT) (Paik, et al., 2013).

For the investigations in this paper, the INSEAN E779A standard test propeller has been selected as a benchmark propeller. This model propeller, which is a four-bladed FPP (Fixed Pitch Propeller) with small skew, was designed in 1959 and was tested by INSEAN (Instituto Nazionale di Studi ed Esperienze di Architettura Navale) in non cavitating and cavitating conditions. The E779A propeller was used in the collaborative EU project VIRTUE and Salvatore et al. (2009) presented the results of

this project in the Rome Workshop including cavitation investigations. The workshop included different computational models i.e. RANS, LES and BEM in comparing non-cavitating and cavitating conditions for propeller performance, including pressure distributions and cavitation patterns. Pereira et al. (2004) conducted numerical and experimental studies in uniform flow for cavitation characteristics on the same propeller. Additionally, Pereira et al. (2006) also carried out a further experimental study in a cavitation tunnel in non-uniform flow. This study described a correlation between cavitation patterns on blades and near field pressures.

In addition to such experimental studies for the E779A propeller, various benchmark simulations have been conducted using CFD methods and comparisons made with the experimental results. For example, Vaz et al. (2015) simulated the E779A propeller using RANS and RANS-BEM coupled approaches in non-cavitating and cavitating conditions for the prediction of propeller performance, pressure distributions and cavitation patterns. Although these simulations succeed in validating the propeller performance and cavitation patterns on the propeller blade surface, the tip vortex cavitation could not be simulated, especially its extension in the propeller's slipstream.

Within the above framework the main focus of this paper is a more accurate simulation of propeller cavitation particularly the tip vortex cavitation and its extension through the rudder domain in order to investigate its interaction with the rudder. The paper first presents details of the theoretical and numerical models used in the CFD code. The geometric details of the benchmark propeller is given in §3. The propeller flow was first simulated with the propeller in isolation, in order to investigate the cavitation phenomenon on the propeller blade surfaces. Details of these simulations for cavitating conditions are presented in §4, including development of the sheet and tip vortex cavitation. After the sheet cavitation has been simulated properly, a new meshing approach is developed using a tube and spiral geometry around propeller tip region to simulate tip vortex cavitation and its trajectories in the propeller's slipstream until the rudder. This is followed by the introduction of the rudder in the slipstream to evaluate interaction between the tip vortex cavitation and the rudder in §5. Concluding remarks including future work are contained in §6.

2. Numerical Method

The cavitation simulations were conducted using CFD methods in the commercial CFD software, Star CCM+. For cavitation simulation, two fluids (water and vapour) were defined in the software and the Volume of Fluid (VOF) method was used. DES and LES turbulence models were preferred for modelling cavitation properly. In contrast to the RANS model, scale-resolving simulations can represent the large scales of turbulence and model small-scale motions. There are two approaches (DES and LES) which are available for scale-resolving simulations in Star CCM+ (Star CCM+ User

Guide, 2018). For this reason, DES and LES models have been preferred more commonly for simulating complex physical phenomenon such as cavitation. For simulating cavitation, the Schnerr-Sauer cavitation model, which is based on Rayleigh Plesset equation, was used in this paper.

In the Schnerr-Sauer model, the bubble growth rate is estimated using Equation 1.

$$(\frac{dR}{dt})^2 = \frac{2}{3}(\frac{p_{sat} - p_\infty}{\rho_l}) \quad (1)$$

The cavitation number based on rotational speed of the propeller is defined as

$$\sigma_n = \frac{p - p_{sat}}{0.5\rho_l(nD)^2} \quad (2)$$

where p is the tunnel pressure, p_{sat} is the vapour pressure, ρ_l is the density of the fluid, n is the rotation rate and D is the diameter of the propeller.

The advance ratio is defined as

$$J = \frac{V_A}{nD} \quad (3)$$

where V_A is the advance velocity of fluid. Thrust and torque coefficient of the propeller is calculated as

$$K_T = \frac{T}{\rho n^2 D^4} \quad (4)$$

$$K_Q = \frac{Q}{\rho n^2 D^5} \quad (5)$$

where T and Q are thrust and torque values of the propeller respectively and ρ is the density of fluid. The propeller open water efficiency is defined as

$$\eta_0 = \frac{J}{2\pi}\frac{K_T}{K_Q} \quad (6)$$

3. Benchmark Propeller

As stated in the introduction, the INSEAN E779A test propeller was used as the benchmark propeller in this study. Figure 1 and Table 1 give the geometry and main particulars of this model propeller, Salvatore et al. (2009).

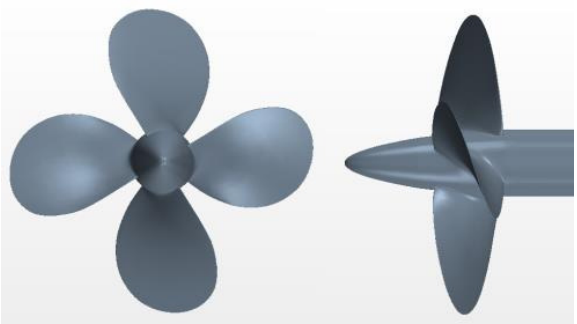

Figure 1. CAD geometry of the benchmark propeller

Table 1. Particulars of the Propellers

Number of Blades (Z)	4
Diameter (D)	0.227m
Pitch Ratio (P/D)	1.1
Area Ratio (A_E/A_0)	0.69

4. Propeller Cavitation

Details of the cavitation simulations including geometry and domain preparation (§ 4.1), mesh generation and settings (§ 4.2) and results (§ 4.3) are presented in this section.

4.1 Domain Preparation and Boundary Conditions

During the simulations two different domains were prepared for the isolated propeller and propeller-rudder interaction cases. For simulating the isolated propeller cavitation, the domain included only the propeller geometry. Figure 2 shows the corresponding domain and boundary conditions.

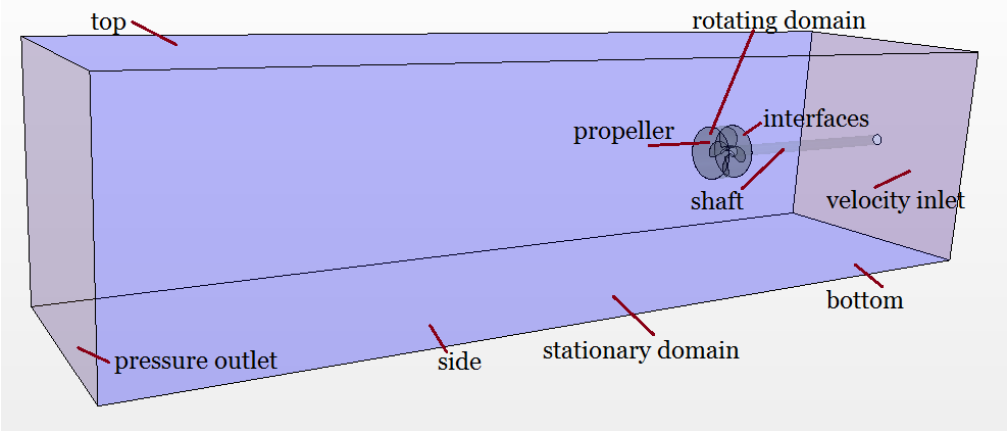

Figure 2. Domain and Boundary Conditions

4.2 Mesh Generation and Simulation Setup

Firstly, the isolated propeller in cavitating condition case was simulated. The cavitation pattern on the propeller blade surfaces (sheet cavitation) was simulated without any mesh refinement approach. Then a tube and spiral geometry was used in a regional mesh refinement approach around the propeller tip

area. The Authors first introduced this approach in a pilot study, which involved an advanced mesh refinement technique by using a tube geometry around propeller's tip region for capturing tip vortex cavitation in a propeller slipstream, in a recent international propeller symposium, SMP'17 (Yilmaz et al. 2017). This technique is the building block of this advanced approach, which is created using a spiral geometry extending the existing tube through the tip vortex trajectories. This section therefore gives a brief summary and results of this pilot study and the new spiral study which enabled a limited extension of the cavitating tip vortex on the benchmark INSEAN E779A propeller which was analysed in cavitating conditions. The results of this analysis were compared with previously published experimental results (Salvatore et al. 2009). First, sheet cavitation was simulated successfully. Then a mesh refinement method was implemented in this analysis using the above mentioned tube geometry and then spiral geometry applied to initiate and extend the tip vortex cavitation in the propeller slipstream. The propeller geometry, simulation settings and brief discussion of this pilot study are summarised below while further details can be found in Yilmaz et al. (2017). Figure 3 shows the tube and spiral geometry used for mesh refinement around the propeller tip region to enable simulation of tip vortex cavitation in propeller's slipstream. Figure 4 illustrates the mesh generated using the tube (Left) and the spiral (Right) geometries for the cavitation simulations. The fine mesh was generated using approximately 0.002D surface size for the refinement area (for tube and spiral geometry) with 12 and 19 million cells for tube and spiral geometry refinement respectively. The average y+ value was around 1 for propeller geometry using 12 prism layers and approximately 1 mm total thickness of prism layer.

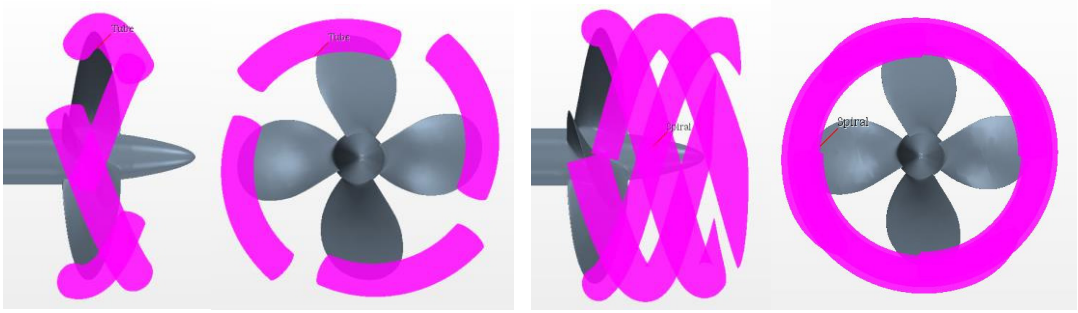

Figure 3. Volumetric Control Region for Mesh Refinement

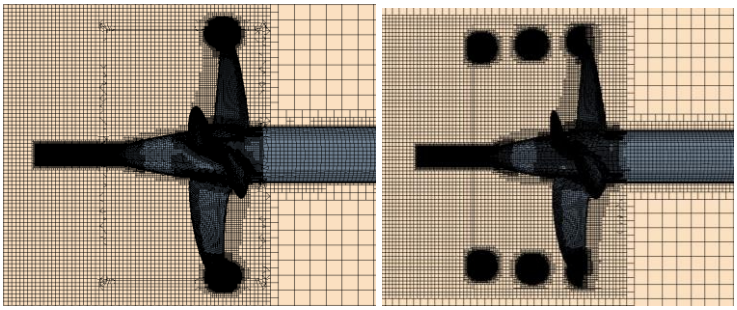

Figure 4. Grid Generation with Volumetric Control Region
(Left; Tube Geometry, Right; Spiral Geometry)

4.3 Results

Results of the cavitation simulations for the propeller in isolation has been represented in terms of the cavitation patterns as well as the propeller performance coefficients in this section. Firstly, the sheet cavitation which has been simulated without any mesh refinement around propeller tip region, is illustrated in section § 4.3.1. Then, tube and spiral geometries were used as a volumetric control to generate a finer mesh around the propeller tip region where the tip vortex cavitation may occur. The results and comparisons for the tip vortex cavitation simulations using the tube and spiral are presented in section § 4.3.2.

4.3.1 Sheet Cavitation

Cavitation was simulated for J=0.71 and σ_n=1.763 solely for the open propeller geometry and compared with experimental results from Salvatore (Salvatore et al. 2009). In general the sheet cavitation patterns computed on the E779A the blade surfaces and at the hub (Figure 5) showed good agreement with Salvatore's experiment images.

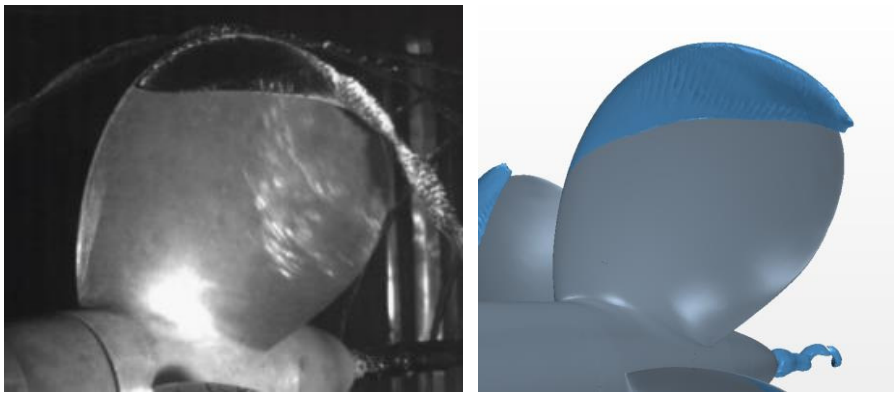

Figure 5. Sheet cavitation comparisons between EFD and CFD, E779A propeller (J=0.71, σ_n=1.763) (Salvatore et al. 2009)

4.3.2 Tip Vortex Cavitation

However, it was concluded that this mesh and analysis method were not sufficient for capturing the extension of a cavitating tip vortex in the propeller slipstream and the existing method still required to be improved to simulate tip vortex cavitation using different methods as well as surface size and refinement of the mesh. For this reason, a helical tube was created around the propeller's tip (Figure 3) to generate a finer mesh in that region. The main purpose of this approach is to create a very fine mesh around tip area where the tip vortex cavitation probably occurs. This technique provided an improvement in the appearance of tip vortex cavitation (Figure 7). It was observed that this improvement is directly related to the mesh size. After creating the helical tube geometry and using it for the mesh refinement, extension of the tip vortex could be simulated and better results (Figure 7) were obtained for the cavitating tip vortex, however, these results still needed to be improved.

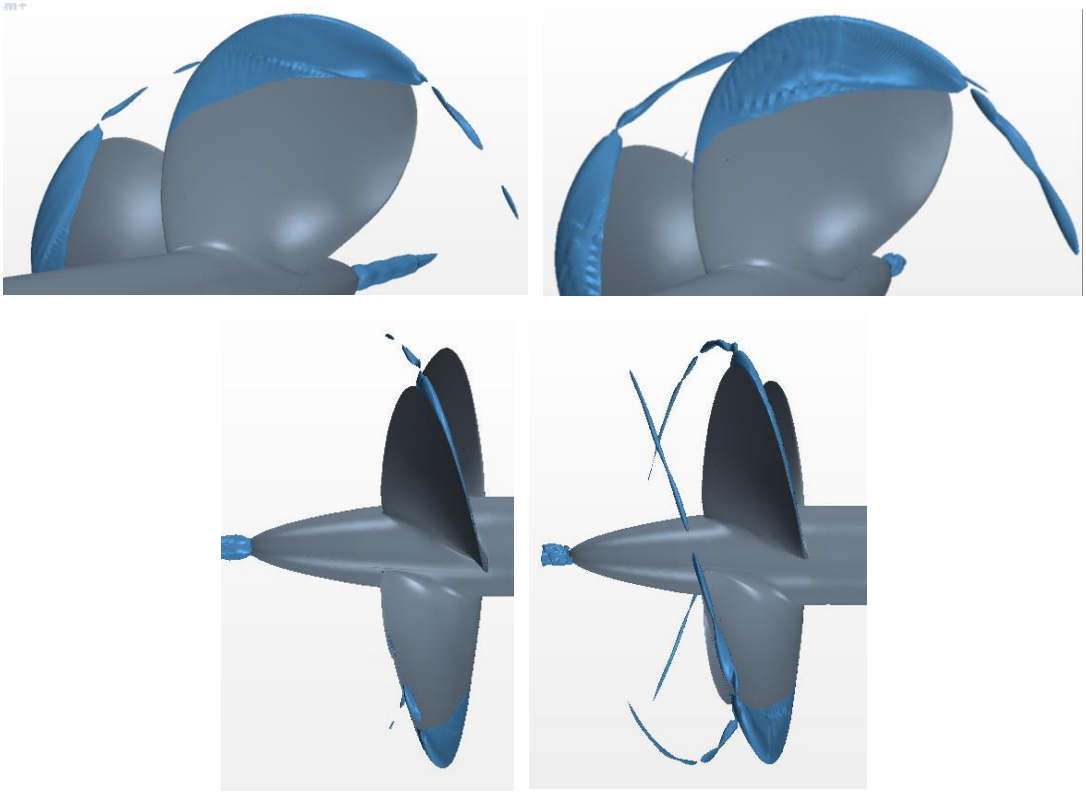

Figure 6. Tip Vortex Cavitation Extension (J=0.71, σ_n=1.763)
(Left; Using Tube Geometry, Right; Using Spiral Geometry)

Table 2. Result Comparison

Performance Coefficient					**Difference (CFD & EFD)**		
Mesh Refinement	**J**	**K_T**	**$10K_Q$**	**η_0**	**K_T**	**$10K_Q$**	**η_0**
Tube	0.71	0.230	0.432	0.601	-10%	-6%	-4%
Spiral	0.71	0.244	0.439	0.627	-4%	-4%	0%
EFD Results	0.71	0.255	0.429	0.626	-	-	-

After evaluating the results and the relationship between mesh size and cavitation extent, the tube geometry was extended in a spiral geometry as shown in Figure 3. By using the tube and spiral geometry around the propeller's tip regions in combination with an adaptive mesh refinement approach results and images were obtained as shown in Figure 6. This approach was considered appropriate for extending the propeller tip vortex cavitation further downstream of the propeller to the rudder and to offer the possibility to investigate its interaction with the rudder.

The improvement was achieved in terms not only of the tip vortex cavitation extension but also the hydrodynamic performance coefficients (K_T, K_Q and η_0) of the propeller. Table 2 shows the comparisons of these coefficients between the CFD results with tube, with spiral and EFD results

respectively. While the tip vortex cavitation has been extended using the spiral geometry, thrust and torque values were also computed closer to the EFD results.

5. Propeller Rudder Interaction

5.1 Geometry Preparation and Boundary Conditions

As stated in the introduction part of the paper, the INSEAN E779A propeller was also tested in the presence of a rudder in its slipstream at the Italian Navy Cavitation Tunnel and associated experimental data was published in (Felli and Falchi, 2011). This experimental set-up was simulated in CFD to compare with the associated experimental data. The rudder geometry was modelled as a 2D wing with a standard symmetric NACA0020 profile section with 180-mm chord and 600-mm span, located behind the propeller geometry as shown in Figure 7.

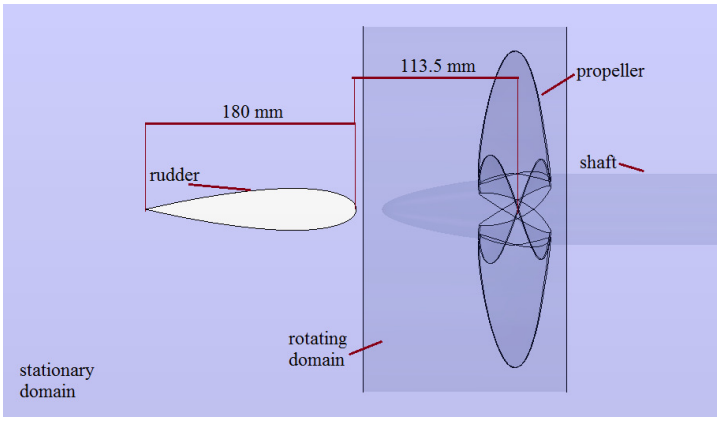

Figure 7. CFD simulation configuration including propeller and rudder geometry

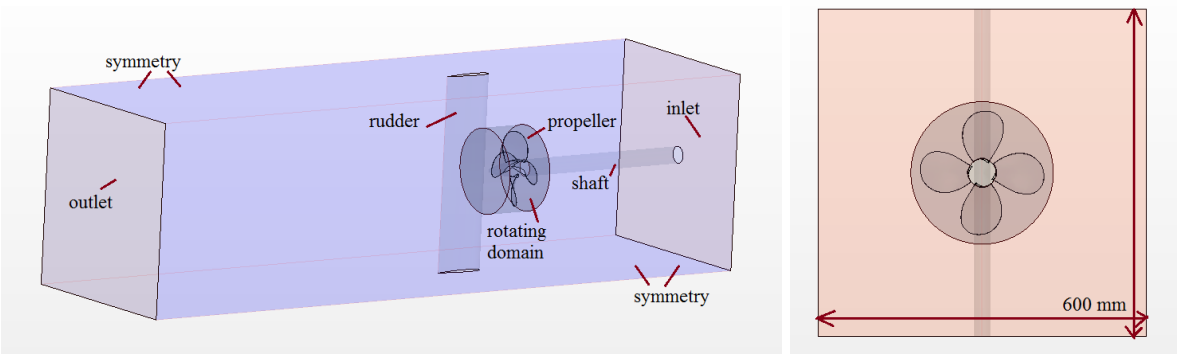

Figure 8. Domain and Boundary Conditions

The domain was prepared in Star CCM+ using the same dimensions of the cavitation tunnel presented in (Felli and Falchi, 2011). The side walls, top and bottom surfaces of the domain have been described as ‘symmetry’ boundary conditions instead of ‘wall’ to prevent numerical errors and divergence problem due to the closeness to the propeller geometry. (Figure 8)

5.2 Mesh Generation and Simulation Setup

The mesh has been generated using the spiral geometry as described in section § 4. Figure 9 shows both the spiral geometry as a control volume and the corresponding generated mesh. The mesh was generated using approximately 0.002D surface size for the refinement area (spiral geometry) with 19 million cells in total.

For the investigations of the propeller-rudder interaction, two different cases have been considered in the following: in the first case (Case 1) the same operating condition has been simulated for the propeller in isolation and for cavitating conditions with J = 0.71 and σ_n = 1.763 (i.e. as in § 4 but in the presence of rudder); in the second case (Case 2) the operating conditions published in (Felli and Falchi, 2011), and shown in Table 3, have been simulated.

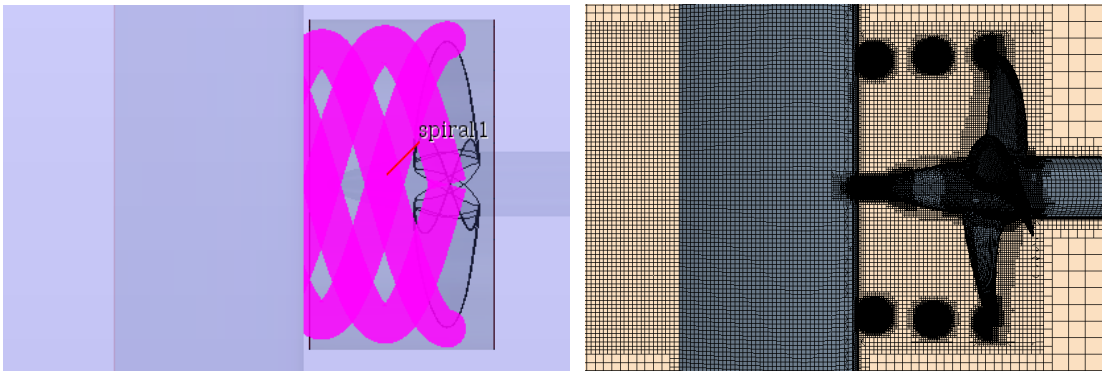

Figure 9. Volumetric Control Region for Mesh Refinement

Table 3. Case Description for Propeller Rudder Interaction

	Propeller - Rudder	
Variables	**Case 1**	**Case 2**
J	0.71	0.88
n	36	25
σ_n	1.763	1.54

5.3 Results

5.3.1 Case 1

For the Case 1 the same condition, which was used for the propeller in isolation, was used in terms of J and σ_n values. To investigate the interaction phenomenon the rudder geometry was introduced behind the propeller the benchmark propeller and the simulation was conducted using the same condition. The earlier described mesh refinement approach was used with the spiral geometry for this simulation. As shown in Figure 10, extension of the tip vortex cavitation has been achieved using this

method in the presence of the rudder but the tip vortex trajectories do not exactly reach the rudder. For this case, a comparison between the DES and LES models was also made in order to evaluate the effect of the turbulence model. For understanding this effect, other simulation parameters and the generated mesh were kept same. It was observed that the LES model gave better results in terms of the tip vortex cavitation extent when the corresponding images were compared as shown in Figure 11.

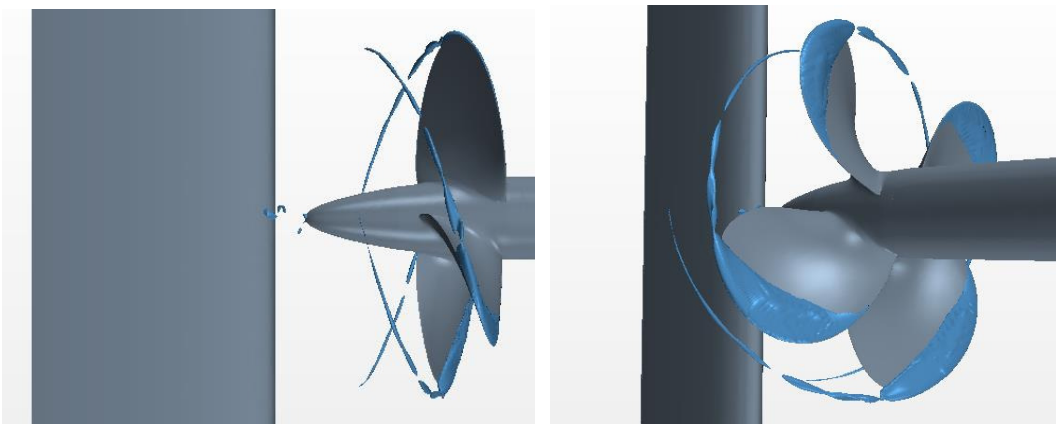

Figure 10. Cavitation pattern including tip vortex cavitation using spiral geometry for mesh refinement ($J=0.71$, $\sigma_n=1.763$)

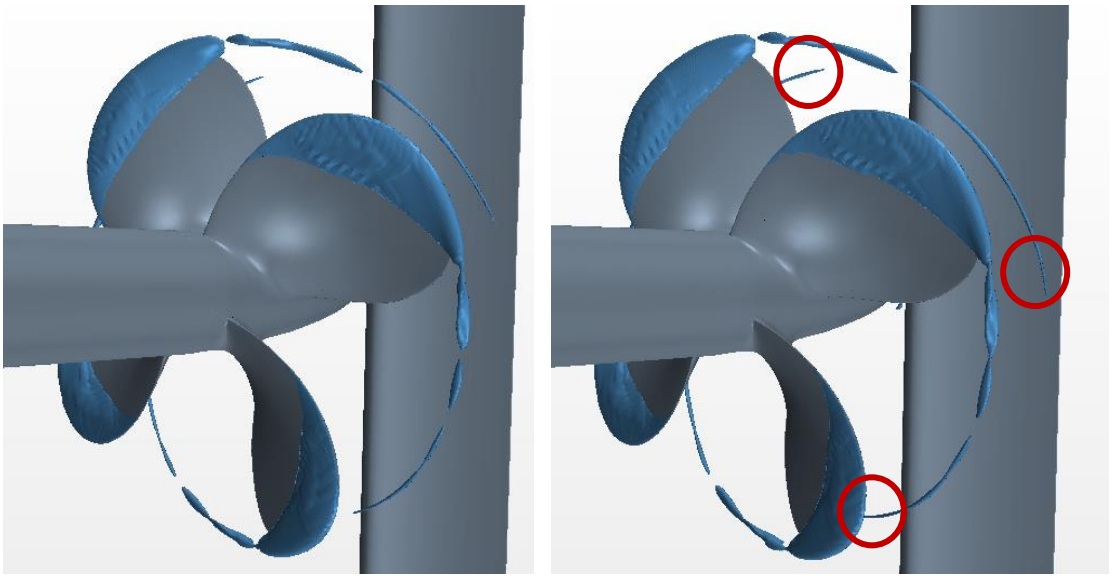

Figure 11. Tip vortex cavitation comparisons between DES and LES models
(Left; DES Model, Right; LES model)

5.3.2 Case 2

To compare the CFD results with the experiments Case 2 was simulated according to the cavitating conditions in (Felli and Falchi, 2011). Although Case 1 showed very good results in terms of the tip vortex cavitation extent, the results were not comparable with the experiments since there were no published data in open literature for this condition. Thus a new case (i.e. Case 2) with different J and σ_n values (as shown in Table 3) was run to compare the CFD simulation results with the experimental ones. Section planes were prepared using the data in the paper as it may be observed in Figure 12 to compare the velocity distributions on section planes and evaluate the flow characteristics. While Figure 13 shows the cavitation pattern obtained from CFD results, Figure 14 and 15 show the comparison between CFD and EFD results for velocity distributions on these section planes. Although the tip vortex cavitation extent could not be simulated as far aft as in Case 1, the comparisons shows encouragingly good agreement with the experiments in terms of velocity distribution. The reason for the difference in the cavitation extents between Case 1 and Case 2 can be explained by the fact that the tip vortex cavitation in Case 2 is not as strong as in Case 1 as a result of the higher J and lower σ. Thus, the existing surface size in spiral mesh refinement area is not sufficiently fine to capture the smaller diameter of the cavitating tip vortex trajectories for Case 2.

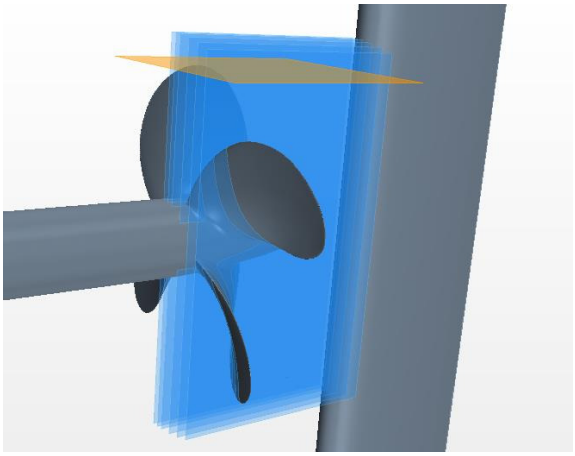

Figure 12. Section planes (y and z planes)

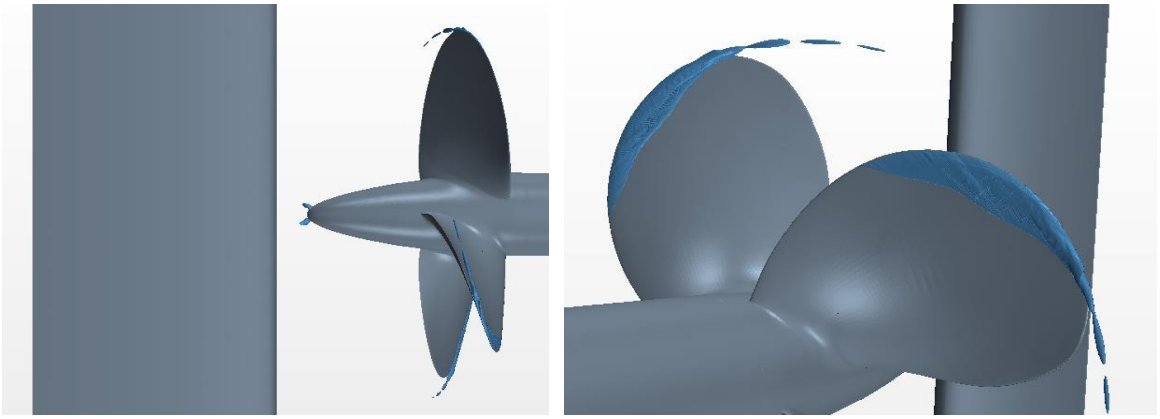

Figure 13. Cavitation pattern including tip vortex cavitation using spiral geometry for mesh refinement (J=0.88, σ_n=1.54)

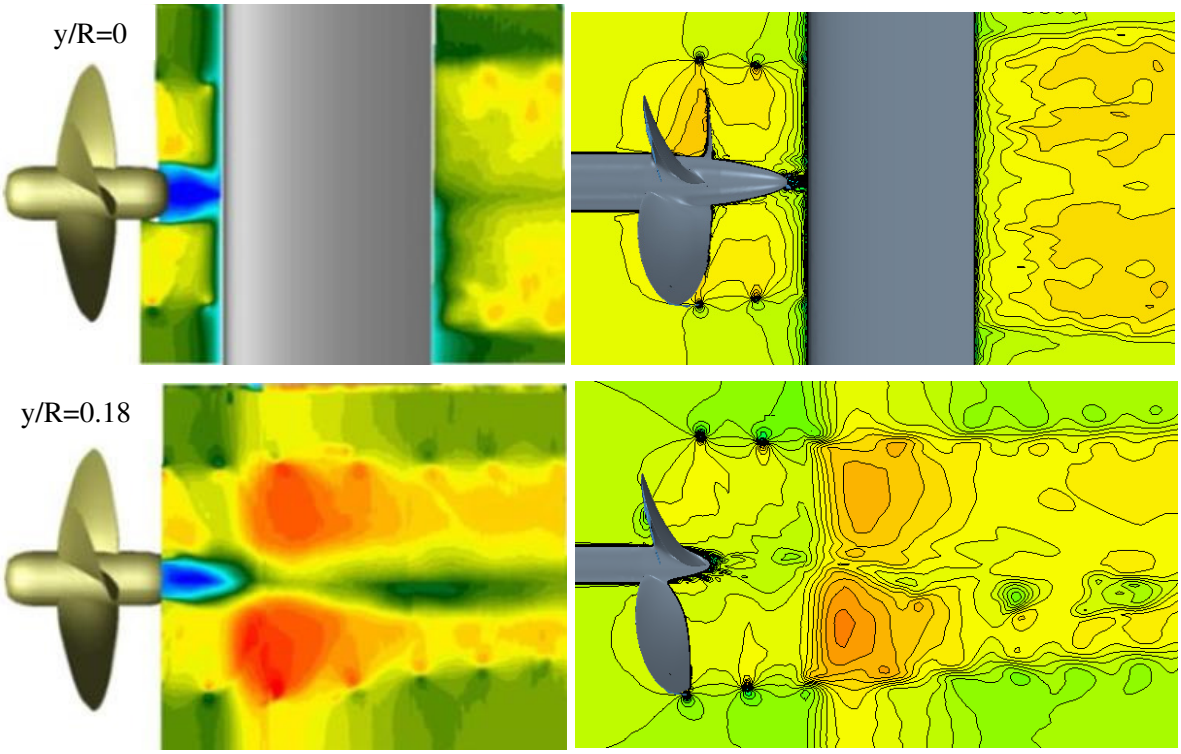

Figure 14. Velocity distribution comparisons between EFD and CFD Results (J=0.88, σ_n=1.54) (Left; EFD Results, Right; CFD Results) (Felli and Falchi, 2011)

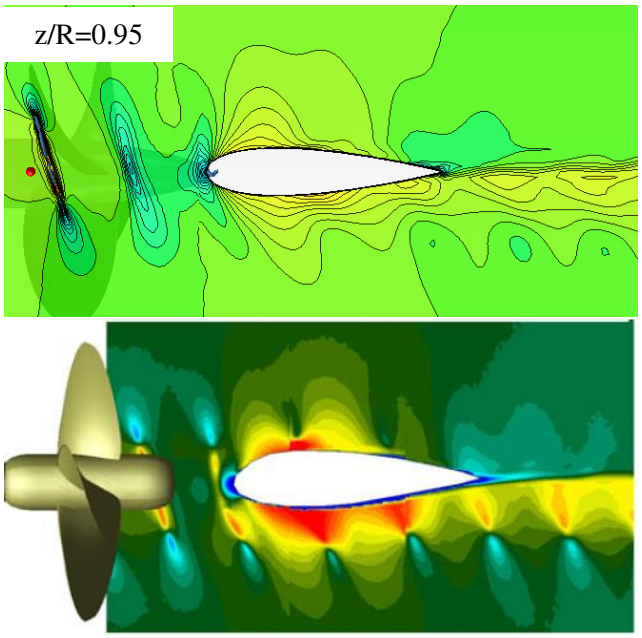

Figure 15. Velocity distribution comparisons between EFD and CFD Results (J=0.88, σ_n=1.54) (Top; CFD Results, Bottom; EFD Results) (Felli and Falchi, 2011)

6. Concluding Remarks

This paper presented cavitation simulations on a model propeller focussing on tip vortex cavitation and its extension into the propeller slipstream through the development of a new spiral mesh refinement method. This approach was used to investigate the propeller-rudder interaction of a cavitating propeller and it was concluded that

- The new method achieved very good correlation in simulating the cavitation characteristics of the INSEAN E779A model propeller in isolation (i.e. in the absence of a rudder in its slipstream)

- The introduction of a rudder behind the same propeller and simulating the propeller cavitation for this arrangement demonstrated the capability of the new method in capturing the tip vortex cavitation trajectories successfully as far aft as the rudder.

- Simulation results from the above arrangement compared favourably with the available experimental data for the same model propeller and indicated that the new method presents encouraging correspondence with the experimental data for the pressure and velocity distributions in the propeller's slipstream and on the rudder. However, the tip vortex cavitation trajectories for this test case did not fully reach the rudder and hence further improvements are required in order to capture the smaller cavitating core of the relatively light loading (Case 2) of the test propeller. This will in turn require smaller cell size and further optimisation of the adaptive meshing technique used. This work is currently in progress, to enable a more detailed study of cavitation-related propeller-rudder interaction.

Acknowledgements

The principal author of this paper is sponsored by the Turkish Ministry of Education during this study. The access provided to High Performance Computing for the West of Scotland (Archie-West) thorough EPSRC grant no. EP/K000586/1 is gratefully acknowledged. The authors are also grateful to CRN-INSEAN, especially Francesco Salvatore, for providing the geometry of the E779A propeller and sharing their experimental data.

References

Boorsma, A., Whitworth, S. (2011). Understanding the Details of Cavitation, Second International Symposium on Marine Propulsors smp'11, Hamburg, Germany, June 2011.

Carlton, J. (2007). Marine Propellers and Propulsion, Elsevier Ltd.

Carlton, J., Radosavljevic, D., Whitworth, S. (2009). Rudder – Propeller – Hull Interaction: The Results of Some Recent Research, In-Service Problems and Their Solutions, First International Symposium on Marine Propulsors smp'09, Trondheim, Norway, June 2009.

Felli, M., Falchi, M. (2011). Propeller tip and hub vortex dynamics in the interaction with a rudder, Exp Fluids DOI 10.1007/s00348-011-1162-7.

Felli, M., Roberto, C., Guj, G. (2008). Experimental analysis of the flow field around a propeller rudder configuration, Exp Fluids (2009) 46:147–164, DOI 10.1007/s00348-008-0550-0.

Han, J. M., Kong, D.S., Song, I. H., Lee, C.S. (2001). Analysis of the cavitating flow around the horn-type rudder in the race of a propeller, CAV2001:sessionB9.005.

Lee, H., Kinnas, S. A., Gu, H., Atarajan, S. (2003). Numerical modeling of rudder sheet cavitation including propeller/rudder interaction and the effects of a tunnel, Fifth International Symposium on Cavitation (CAV2003) Osaka, Japan, November 1-4, 2003.

Natarajan, S. (2003). Computational Modelling of Rudder Cavitation and Propeller/Rudder Interaction, Master Dissertation, The University of Texas at Austin.

Paik, K. J., Park, H. G., Seo, J. (2013). RANS simulation of cavitation and hull pressure fluctuation for marine propeller operating behind-hull condition, Int. J. Nav. Archit. Ocean Eng. (2013) 5:502~512 pISSN: 2092-6782, eISSN: 2092-6790.

Pereira, F., Felice, F. D., Salvatore, F. (2016). Propeller Cavitation in Non-Uniform Flow and Correlation with the Near Pressure Field, Journal of Marine Science and Engineering, 4, 70; doi:10.3390/jmse4040070.

Pereira, F., Salvatore, F., Felice, F. D. (2004). Measurement and Modeling of Propeller Cavitation in Uniform Inflow, Journal of Fluids Engineering, Vol. 126.

Salvatore, F., Streckwall, H., Terwisga, T. (2009). Propeller Cavitation Modelling by CFD- Results from the VIRTUE 2008 Rome Workshop, First International Symposium on Marine Propulsors smp'09, Trondheim, Norway.

Star CCM+ User Guide, (2018).

Szantyr, J. A. (2007a). Mutual hydrodynamic interaction between the operating propeller and the rudder, Archives of Civil and Mechanical Engineering, Vol. VII 2007 No. 3.

Szantyr, J. A. (2007b). Dynamic interaction of the cavitating propeller tip vortex with the rudder, Polish Maritime Research 4(54) 2007 Vol 14; pp. 10-14 DOI: 10.2478/v10012-007-0033-x

Vaz, G., Hally, D., Huuva, T., Bulten, N., Muller, P., Becchi, P., Herrer, J., Whitworth S., Mace, R., Korsström, A. (2015). Cavitating Flow Calculations for the E779A Propeller in Open Water and Behind Conditions: Code Comparison and Solution Validation, Fourth International Symposium on Marine Propulsors smp'15, Austin, Texas, USA.

Yilmaz, N., Khorasanchi, M., Atlar, M. (2017). An Investigation into Computational Modelling of Cavitation in a Propeller's Slipstream, Fifth International Symposium on Marine Propulsion smp'17, Espoo, Finland, June 2017.